Journal of Physics: Conference Series **124** (2008) 012029 doi:10.1088/1742-6596/124/1/012029

Reconstructions of Piecewise Constant Conductivities by the D-bar Method for Electrical Impedance Tomography

Kim Knudsen[1], Matti Lassas[2], Jennifer Mueller[3] and Samuli Siltanen[4]

[1] Department of Mathematical Sciences, Aalborg University, Denmark, [2] Institute of Mathematics, Helsinki University of Technology, Finland, [3] Department of Mathematics, Colorado State University, Colorado and School of Biomedical Engineering, Colorado State University, Colorado, [4] Samuli Siltanen, Institute of Mathematics, Tampere University of Technology, Finland

E-mail: [1] kim@math.aau.dk, [2] mjlassas@math.hut.fi, [3] mueller@math.colostate.edu, [4] samuli.siltanen@tut.fi

Abstract. The importance of the solution of the boundary integral equation for the exponentially growing solutions to the Schrödinger equation arising from the 2-D inverse conductivity problems is demonstrated by a study of reconstructions of simple piecewise constant conductivities on a disk from two methods of approximating the scattering transform in the D-bar method and from Calderón's linearization method.

1. Introduction

The inverse conductivity problem was posed by Calderón in the seminal paper [8] and it concerns the unique determination and reconstruction of an isotropic conductivity distribution in a bounded domain from electrostatic measurements on the boundary of the domain. This problem is the mathematical problem behind the technology for medical imaging known as electrical impedance tomography (EIT) (see [9, 5] for review articles on EIT). Conductivity distributions appearing in applications are typically piecewise continuous. This is the case for example in medical EIT, since various tissues in the body have different conductivities with discontinuities at organ boundaries. Here we consider 2-D reconstructions. These can be used to image cross-sections of a 3-D region, such as a patient's torso. In the case of patients receiving mechanical ventilation, for example, 2-D cross-sections are useful for obtaining regional ventilation information in the lungs, which is valuable for setting and controlling the airflow and pressure settings on the ventilator [25, 1]. Real-time imaging of cross-sectional lung activity can also be used for diagnostic purposes, such as detecting a lung collapse, a pulmonary embolism, pulmonary edema, or a pneumothorax.

To state the problem formally, let $\Omega \subset \mathbb{R}^2$ be a bounded domain with smooth boundary $\partial\Omega$ and let $\gamma \in L^\infty(\Omega)$ be the conductivity distribution in Ω satisfying

$$C^{-1} < \gamma(x) < C, \quad x \in \Omega \tag{1}$$

for some constant $C > 0$. Putting a voltage potential $f \in H^{1/2}(\partial\Omega)$ on the boundary gives rise to an electric potential $u \in H^1(\Omega)$ inside Ω described as the unique solution to the Dirichlet problem

$$\nabla \cdot \gamma \nabla u = 0 \quad \text{in} \quad \Omega, \qquad\qquad u|_{\partial\Omega} = f. \tag{2}$$

The current flux through the boundary is given by the quantity $\gamma \partial_\nu u$, where ν is the outer unit normal to the boundary. Thus the measurements at the boundary are described by the Dirichlet-to-Neumann map (voltage-to-current map)

$$\begin{aligned} \Lambda_\gamma \colon H^{1/2}(\partial\Omega) &\to H^{-1/2}(\partial\Omega) \\ f &\mapsto \gamma \partial_\nu u. \end{aligned}$$

The associated quadratic form

$$Q_\gamma(f) = \langle f, \Lambda_\gamma f \rangle = \int_\Omega \gamma |\nabla u|^2 dx,$$

where u solves (2), represents the power needed to maintain the voltage f at the boundary. In this formalism Calderón's problem is to show that the map $\gamma \mapsto \Lambda_\gamma$ is injective and furthermore to find an algorithm for the inversion of the map.

Let us briefly outline the main results on the inverse conductivity problem. In [8] Calderón solved the linearized problem and proposed a linearized reconstruction algorithm. (See [10, 26, 27, 16] for other work on Calderón's method.) Then in [17, 18] Kohn and Vogelius proved uniqueness for piecewise real-analytic conductivities. In three dimensions a major breakthrough was in [24], where Sylvester and Uhlmann showed uniqueness for smooth conductivities using exponentially growing solutions. The assumptions have since been relaxed in [6, 21]. For the two-dimensional problem considered here Nachman gave a constructive uniqueness proof for smooth conductivities in [20]. The assumptions have since been relaxed [7, 14, 13]. A final answer was recently given by Astala and Päivärinta [2] for merely bounded conductivities. See also [3].

The D-bar method proposed is a reconstruction algorithm which follows from the constructive uniqueness proof in [20]. The method is based on exponentially growing solutions $\psi(x, k)$ to the conductivity equation (2), see Section 2 below. Their traces on $\partial\Omega$ satisfy the equation

$$A_\gamma \psi(\cdot, k)|_{\partial\Omega} = e^{ikx}, \tag{3}$$

where

$$A_\gamma = I + S_k(\Lambda_\gamma - \Lambda_1).$$

Here S_k is the single-layer operator

$$(S_k \phi)(x) := \int_{\partial\Omega} G_k(x - y)\phi(y) d\sigma(y), \quad k \in \mathbb{C} \setminus 0, \tag{4}$$

with $G_k(x)$, the Faddeev's Green's function, defined by

$$G_k(x) := \frac{e^{ikx}}{(2\pi)^2} \int_{\mathbb{R}^2} \frac{e^{ix\cdot\xi}}{|\xi|^2 + 2k(\xi_1 + i\xi_2)} d\xi.$$

The dot product is computed with real vectors $x = (x_1, x_2)$ and $\xi = (\xi_1, \xi_2)$. The equation (3) is a uniquely solvable Fredholm equation of the second kind. As we will explain in the following

section, the so-called *scattering transform* provides an important link between the measured data and the reconstructed conductivity. In terms of the measured data this function is defined by

$$\mathbf{t}(k) = \int_{\partial\Omega} e^{i\overline{k}\overline{x}}(\Lambda_\gamma - \Lambda_1)\psi(\cdot,k)d\sigma(x), \qquad k \in \mathbb{C},\ x = x_1 + ix_2. \tag{5}$$

To reconstruct the conductivity from $\mathbf{t}$ one has to solve a D-bar equation with respect to the k variable, see Section 2.

Since solving (3) is severely ill-posed, in [22] a simple approximation for the scattering transform is introduced in which we replace $\psi|_{\partial\Omega}$ by $e^{ikx}|_{\partial\Omega}$. This approximation denoted by $\mathbf{t}^{\exp}$ was studied further in [16] and used on experimental data in [11, 12]. The ill-posedness of the inverse problem is manifested in the computation of the scattering transform.

Calderón's linearization method can be seen as an approximation of the D-bar method via three linearizations [16]; see Section 2.4 for details. In contrast, the implementation of the D-bar method with the $\mathbf{t}^{\exp}$ approximation only makes one linearizing assumption in the approximation of the scattering transform. Reconstructions of a radially symmetric piecewise constant conductivity with a single jump discontinuity were computed in [16] by both the D-bar method with the $\mathbf{t}^{\exp}$ approximation and by Calderón's method using explicit reconstruction formulas. The reconstructions were very similar in terms of the reconstructed current amplitude and their qualitative features. Even more marked similarities can be found by comparing the results of the D-bar method on experimental tank data in [11] or on human chest data in [12] with the results in [4]. These results suggest that linearizations in the scattering transform have a strong effect on the reconstructed conductivity.

A second method of approximating the scattering transform, denoted $\mathbf{t}^{\mathrm{B}}$, was introduced in [19]. In this method approximations of the traces of the exponentially growing solutions are computed using the standard Green's function for the Laplacian in place of the Faddeev Green's function in (3), and then $\mathbf{t}^{\mathrm{B}}$ is computed using these approximate traces instead of $\psi|_{\partial\Omega}$ in the integral formula for $\mathbf{t}(k)$. Numerical experiments were performed on simulated smooth conductivities with and without noise. In each case the reconstructions resulted in a more accurate amplitude and spatial resolution. This motivates the study of $\mathbf{t}^{\mathrm{B}}$ applied to piecewise constant conductivity distributions conducted here.

The outline of the paper is as follows. In Section 2 we describe in detail the D-bar method. Further, we discuss the three approximation algorithms. The first one uses $\mathbf{t}^{\exp}$, the second one uses $\mathbf{t}^{\mathrm{B}}$, and the third one is Calderón's linearization algorithm. In Section 3 we describe the numerical implementations of the algorithms and test the algorithms on different examples. Finally in Section 4 we discuss the results and conclusions.

2. Reconstruction algorithms

2.1. D-bar reconstruction

The D-bar reconstruction algorithm consists of the two steps

$$\Lambda_\gamma \to \mathbf{t} \to \gamma. \tag{6}$$

In order to compute $\mathbf{t}$ from Λ_γ by (5) one needs to find the trace of $\psi(\cdot,k)$ on $\partial\Omega$.

To compute γ from $\mathbf{t}$ the key observation is that with respect to the parameter k, the function $\mu(x,k) = e^{-ixk}\psi(x,k)$ satisfies for fixed $x \in \mathbb{C}$ the D-bar equation

$$\overline{\partial}_k\mu(x,k) = \frac{1}{4\pi\overline{k}}\mathbf{t}(k)e_{-x}(k)\overline{\mu(x,k)}, \quad k \in \mathbb{C}, \tag{7}$$

where the unimodular function e_k is defined by

$$e_x(k) := e^{i(kx+\overline{k}\overline{x})} = e^{-i(-2k_1,2k_2)\cdot x}. \tag{8}$$

It is shown in [20] (see also [7, 14]) that $\mu(x,\cdot)$ is in fact the unique solution to (7) defined by the asymptotic condition $\mu(x,\cdot) - 1 \in L^r(\mathbb{R}^2), r > 2/\epsilon$. Moreover, the solution belongs to $C^\alpha(\mathbb{R}^2)$ with $\alpha < 1$. Hence $\mu(x,k)$ can be computed from $\mathbf{t}$ by solving (7) or equivalently the Fredholm integral equation

$$\mu(x,s) = 1 + \frac{1}{(2\pi)^2}\int_{\mathbb{R}^2} \frac{\mathbf{t}(k)}{(s-k)\overline{k}} e_{-x}(k)\overline{\mu(x,k)}dk_1dk_2. \tag{9}$$

Finally, the conductivity can be recovered from μ using the formula

$$\gamma(x) = \mu(x,0)^2, \quad x \in \Omega. \tag{10}$$

2.2. D-bar method using $\mathbf{t}^{\exp}$

The approximation $\mathbf{t}^{\exp}$ is defined by substituting $e^{ikx}|_{\partial\Omega}$ for $\psi|_{\partial\Omega}$ in (5) and computing

$$\mathbf{t}^{\exp}(k) = \int_{\partial\Omega} e^{i\bar{k}\bar{x}}(\Lambda_\gamma - \Lambda_1)e^{ikx}d\sigma(x). \tag{11}$$

Since $\mathbf{t}^{\exp}$ grows like $|k|^{1/2}$ as $|k| \to \infty$ [16], the approximate scattering transform $\mathbf{t}^{\exp}$ is restricted to a disk of radius R in the complex plane

$$\mathbf{t}^{\exp}_{\mathrm{R}}(k) = \begin{cases} \mathbf{t}^{\exp}(k), & |k| < R, \\ \mathbf{t}^{\exp}(k)\chi_R(|k|), & |k| \geq R. \end{cases} \tag{12}$$

Here $\chi_R(|k|)$ is either a hard or soft cut-off function near $|k| = R$. Then $\mathbf{t}$ is replaced by $\mathbf{t}^{\exp}_{\mathrm{R}}$ in (9) and we solve

$$\mu^{\exp}_{\mathrm{R}}(x,s) = 1 + \frac{1}{(2\pi)^2}\int_{\mathbb{R}^2} \frac{\mathbf{t}^{\exp}_{\mathrm{R}}(k)}{(s-k)\overline{k}} e_{-x}(k)\overline{\mu^{\exp}_{\mathrm{R}}(x,k)}dk_1dk_2. \tag{13}$$

and compute the reconstruction

$$\gamma^{\exp}_{\mathrm{R}}(x) = \mu^{\exp}_{\mathrm{R}}(x,0)^2.$$

2.3. D-bar method using $\mathbf{t}^{\mathrm{B}}$

In the approach introduced in [19], the Faddeev Green's function in (4) is replaced by the standard Green's function for the Laplacian $G_0(x) := -(2\pi)^{-1}\log|x|$. This is tantamount to dropping a smooth but exponentially growing term in the kernel of S_k. Since the operator

$$A^{\mathrm{B}}_\gamma := I + S_0(\Lambda_\gamma - \Lambda_1)$$

is invertible in $H^{1/2}(\partial\Omega)$ [23], we can define

$$\psi^{\mathrm{B}}(\cdot,k)|_{\partial\Omega} = (A^{\mathrm{B}}_\gamma)^{-1}e^{ikx} \tag{14}$$

and compute the approximation $\mathbf{t}^{\mathrm{B}}$ for $\mathbf{t}$ from the formula

$$\mathbf{t}^{\mathrm{B}}(k) = \int_{\partial\Omega} e^{i\bar{k}\bar{x}}(\Lambda_\gamma - \Lambda_1)\psi^{\mathrm{B}}(\cdot,k)d\sigma. \tag{15}$$

Since $\mathbf{t}^{\mathrm{B}}$ also blows up as $|k| \to \infty$ we cut-off as before and define

$$\mathbf{t}^{\mathrm{B}}_{\mathrm{R}}(k) = \begin{cases} \mathbf{t}^{\mathrm{B}}(k), & |k| < R, \\ \mathbf{t}^{\mathrm{B}}(k)\chi_R(|k|), & |k| \geq R. \end{cases} \tag{16}$$

This approximation is then used as before in the D-bar equation and gives

$$\mu_{\mathrm{R}}^{\mathrm{B}}(x,s) = 1 + \frac{1}{(2\pi)^2}\int_{\mathbb{R}^2} \frac{\mathbf{t}_{\mathrm{R}}^{\mathrm{B}}(k)}{(s-k)\overline{k}} e_{-x}(k)\overline{\mu_{\mathrm{R}}^{\mathrm{B}}(x,k)}dk_1dk_2. \tag{17}$$

Solving the equation gives us the reconstruction

$$\gamma_{\mathrm{R}}^{\mathrm{B}}(x) = \mu_{\mathrm{R}}^{\mathrm{B}}(x,0)^2.$$

2.4. Calderon's method

Calderón's reconstruction method solves the linearized inverse conductivity problem. That is, it assumes the conductivity is a small perturbation from a constant. Let us briefly outline the method in the context of the D-bar method, as derived in [16]. The starting point is again the truncated approximate scattering transform $\mathbf{t}_{\mathrm{R}}^{\mathrm{exp}}$ defined by (12), but instead of solving the D-bar equation and squaring the result, the conductivity is reconstructed according to the formula

$$\gamma^{\mathrm{app}}(x) = 1 - \frac{2}{(2\pi)^2}\int_{\mathbb{R}^2} e_{-x}(k)\frac{\mathbf{t}_{\mathrm{R}}^{\mathrm{exp}}(k)}{|k|^2}dk_1dk_2. \tag{18}$$

The derivation in terms of the D-bar method is given in [16] where it was found that Calderón's method can be put in the context of the D-bar method through three linearizing steps:

(i) Approximate the scattering transform by $\mathbf{t}_{\mathrm{R}}^{\mathrm{exp}}(k)$ defined by (12)

(ii) Approximate the function $\mu_{\mathrm{R}}^{\mathrm{exp}}$ in the integral in the right hand side of (13) by its asymptotic value $\mu_{\mathrm{R}}^{\mathrm{exp}} \sim 1$.

(iii) Linearize the square function in (10): $(1-h)^2 \sim 1 - 2h$.

In contrast, the D-bar method using $\mathbf{t}_{\mathrm{R}}^{\mathrm{exp}}$ makes only the first approximation.

3. Numerical implementation and results

We revisit the nine simple piecewise constant radially symmetric conductivities with a single jump discontinuity studied in [16]. Small, medium, and high contrast conductive disks of small, medium and large radii were reconstructed using D-bar with the $\mathbf{t}_R^{\mathrm{exp}}$ approximation and Calderón's method. We illustrate the improvement in the reconstructions by using $\mathbf{t}_R^{\mathrm{B}}$ in figure 1. Resistive disks of small, medium, and high contrast at the same radii are also studied with reconstructions included in figure 2. In addition, we consider two piecewise constant examples of low and medium contrast with radially symmetric conductivities with two jump discontinuities. The reconstructions are found in figure 3.

The solution of the D-bar equation (9) was computed using the method in [15] at the equally spaced reconstruction points in $[0,1]\times[0,1]$ intersect Ω with spacing 0.01. The truncation radius in the k-plane for the scattering transform was at $R = 15$, except where noted. Note that the D-bar method is mesh-independent in the spatial variable because the D-bar equation is solved for each x in the region of interest to obtain $\gamma(x)$. The method in [15] is a multigrid method based on a method by Vainikko [28] for convolution equations such as those of Lippmann-Schwinger type. The truncation radius R was chosen empirically as large as possible based on the blow-up of $\mathbf{t}_R^{\mathrm{exp}}$ (see [16] for further analysis of the properties of $\mathbf{t}^{\mathrm{exp}}$) and was taken to be the same for $\mathbf{t}_R^{\mathrm{B}}$ for purposes of comparison in the single-jump examples, although $\mathbf{t}_R^{\mathrm{B}}$ could be computed on a disk of larger radius, as in the two-jump examples, resulting in more accurate reconstructions. In the simulations, it is assumed that Λ_γ can be approximated by a matrix acting on the Fourier basis. The Dirichlet-to-Neumann map Λ_1 and Neumann-to-Dirichlet map R_1 corresponding to the homogeneous conductivity 1 have the following form in the trigonometric basis:

$$\Lambda_1\phi_n = |n|\phi_n, \qquad R_1\phi_n = |n|^{-1}\phi_n, \qquad n \in \mathbb{Z}\setminus 0. \tag{19}$$

In addition, $\Lambda_1\phi_0 = 0$, and $R_1\phi_0$ is not defined. When Ω is the unit disc we have the identity $2S_0 = R_1$, see [23]. We thus have a representation of the operator A_γ^{B} in the Fourier basis. The computation of $\psi^{\mathrm{B}}|_{\partial\Omega}$ from (14) is done by performing the convolution on the Fourier side as a multiplication, transforming back, and forming a linear system, which is solved by GMRES. The approximate scattering transform is also computing by performing the convolution on the Fourier side and transforming back, then approximating the integral with a simple Simpson's rule.

Calderón's reconstruction method based on (18) is implemented using the precomputed $\mathbf{t}_{\mathrm{R}}^{\exp}$. As before we have truncated at $R = 15$. The integrand in the right hand side of (18) is computed on an equispaced k-grid in $[-R, R]\times[-R, R]$ of size $2^7\times 2^7$, and the integral is then approximated by a left Riemann sum.

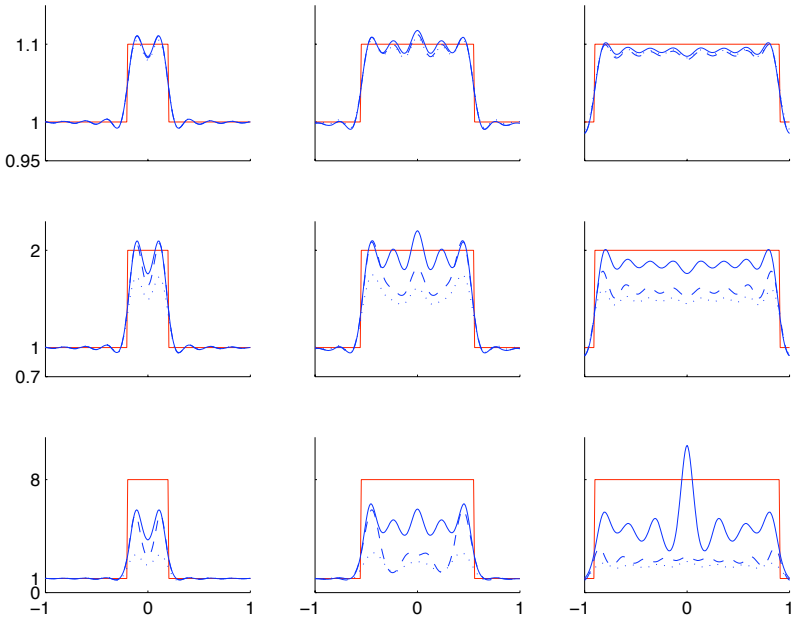

Figure 1. Actual (red) and reconstructed conductivity profiles from Calderón's method (dotted), $\mathbf{t}_R^{\exp}$ (dashed) and $\mathbf{t}_R^{\mathrm{B}}$ (solid) with $R = 15$ for the conductive discontinuous examples. The last two reconstructions in the third row were computed with $R = 12$.

4. Conclusions

Our numerical experiments suggest that the D-bar method using $\mathbf{t}^{\exp}$ and Calderón's linearization method produce quite similar reconstructions, while Calderón's method is computationally faster. Both of these methods have difficulties recovering the amplitude of high contrast conductivities.

The use of an (approximate) integral equation for solving the traces of exponentially growing solutions is found to improve reconstructions: the D-bar method using $\mathbf{t}^{\mathrm{B}}$ recovers extreme conductivity amplitudes and locations of jumps significantly better than the two other methods.

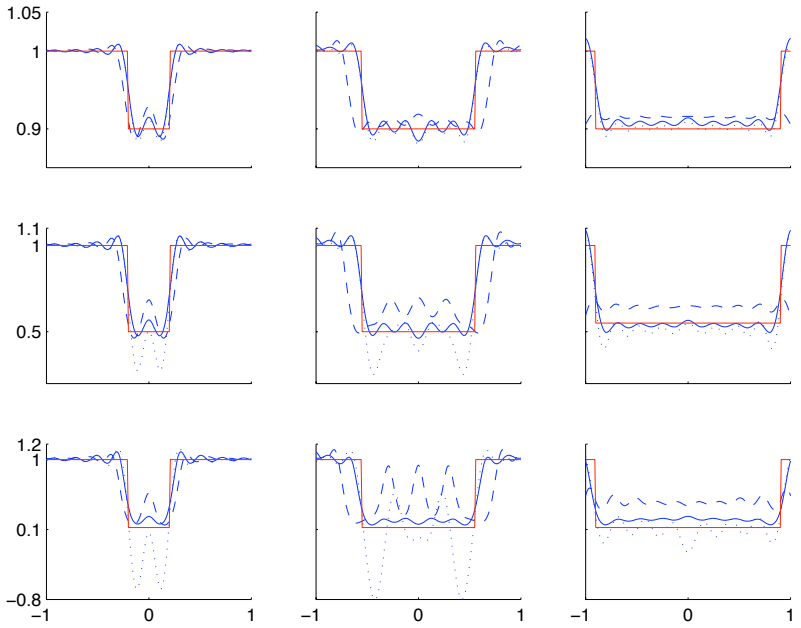

Figure 2. Actual (red) and reconstructed conductivity profiles from Calderón's method (dotted), $\mathbf{t}_R^{\exp}$ (dashed) and $\mathbf{t}_R^{\mathrm{B}}$ (solid) with $R = 15$ for the resistive discontinuous examples. The last reconstruction in the third row was computed with $R = 12$. Note that the last row of examples has the highest contrast; the scale of the plots were chosen to accomodate the Calderón reconstructions.

Acknowledgments

The work of JM was supported by the National Science Foundation under Grant No. 0513509. The work of KK was supported by a grant from the Danish Research Council for Technology and Production. The work of ML and SS was supported by the Academy of Finland (Finnish Programme for Centres of Excellence in Research 2006-2011, application number 213476).

References

[1] M. B. P. Amato, C. S. Barbas, D. M. Medeiros, R. B. Magaldi, G. P. Schettino, G. Lorenzi-Filho, R. A. Kairalla, D. Deheinzelin, C. Morais, E. O. Fernandes, T. Y. Takagaki, and C. R. R. Carvalho, *Effect of a protective-ventilation strategy on mortality in the acute respiratory distress syndrome*, N Engl J Med, 338 (1998), pp.347–354.

[2] K. Astala and L. Päivärinta, *Calderón's inverse conductivity problem in the plane*, Ann. of Math., 163 (2006), pp. 265–299.

[3] K. Astala, M. Lassas and L. Päivärinta, *Calderón's inverse problem for anisotropic conductivity in the plane*, Comm. Partial Differential Equations, 30 (2005), pp. 207–224.

[4] J. Bikowski and J. L. Mueller, *2D EIT reconstructions using Calderón's method*, preprint, (2007).

[5] L. Borcea, *Electrical impedance tomography*, Inverse Problems, 18 (2002), pp. 99–136.

[6] Russell M. Brown and Rodolfo H. Torres. Uniqueness in the inverse conductivity problem for conductivities with 3/2 derivatives in L^p, $p > 2n$. *J. Fourier Anal. Appl.*, 9(6):563–574, 2003.

[7] R. M. Brown and G. Uhlmann, *Uniqueness in the inverse conductivity problem for nonsmooth conductivities in two dimensions*, Comm. Partial Differential Equations 22 (1997), pp. 1009–1027.

[8] A. P. Calderón, *On an inverse boundary value problem*, In Seminar on Numerical Analysis and its Applications to Continuum Physics, Soc. Brasileira de Matemàtica (1980), pp.65–73.

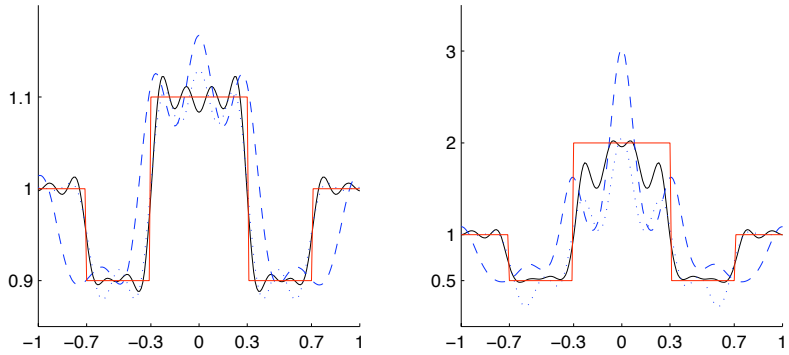

Figure 3. Actual (red) and reconstructed conductivity profiles from Calderón's method with $R = 15$ (dotted), $\mathbf{t}^{\exp}_{R=15}$ (blue dashed) and $\mathbf{t}^{\mathrm{B}}_{R=20}$ (black solid) for the discontinuous examples. Note that the example on the right has the higher contrast.

[9] M. Cheney, D. Isaacson and J. C. Newell, *Electrical Impedance Tomography*, SIAM Review, 41 (1999), pp. 85–101.
[10] D. Isaacson and E. L. Isaacson, *Comment on Calderón's Paper: "On an Inverse Boundary Value Problem"*, Math. of Comp., 52 (1989), pp. 553–559.
[11] D. Isaacson, J. L. Mueller, J. C. Newell, and S. Siltanen, *Reconstructions of chest phantoms by the D-bar method for electrical impedance tomography*, IEEE Trans. Med. Im., 23 (2004) pp. 821–828.
[12] D. Isaacson, J. L. Mueller, J. C. Newell, and S. Siltanen, *Imaging cardiac activity by the D-bar method for electrical impedance tomography*, Physiol. Meas., 27 (2006), pp. S43–S50.
[13] K. Knudsen, *A new direct method for reconstructing isotropic conductivities in the plane,* Physiol. Meas., 24 (2003), pp. 391–401.
[14] K. Knudsen and A. Tamasan, *Reconstruction of less regular conductivities in the plane*, Comm. Partial Differential Equations, 29 (2004), pp. 361–381.
[15] K. Knudsen, J. L. Mueller and S. Siltanen, *Numerical solution method for the D-bar-equation in the plane*, J. Comp. Phys., 198 (2004), pp. 500–517.
[16] K. Knudsen, M. J. Lassas, J. L. Mueller and S. Siltanen, *D-bar method for electrical impedance tomography with discontinuous conductivities*, SIAM J. Appl. Math., (2006).
[17] Robert V. Kohn and Michael Vogelius, *Determining conductivity by boundary measurements*, Comm. Pure Appl. Math. **37** (1984), no. 3, 289–298.
[18] Robert V. Kohn and Michael Vogelius, *Determining conductivity by boundary measurements. II. Interior results*, Comm. Pure Appl. Math. **38** (1985), no. 5, 643–667.
[19] J. L. Mueller and S. Siltanen, *Direct reconstructions of conductivities from boundary measurements*, SIAM J. Sci. Comp., 24 (2003), pp. 1232–1266.
[20] A. I. Nachman, *Global uniqueness for a two-dimensional inverse boundary value problem*, Ann. of Math. 143 (1996), pp. 71–96.
[21] Lassi Päivärinta, Alexander Panchenko, and Gunther A. Uhlmann. Complex geometrical optics solutions for Lipschitz conductivities. *Rev. Mat. Iberoamericana*, 19(1):56–72, 2003.
[22] S. Siltanen, J. Mueller and D. Isaacson, *An implementation of the reconstruction algorithm of A. Nachman*

for the 2-D inverse conductivity problem, Inverse Problems 16 (2000), pp. 681–699.

[23] S. Siltanen, J. Mueller and D. Isaacson *Errata: An implementation of the reconstruction algorithm of A. Nachman for the 2-D inverse conductivity problem,* Inverse Problems

[24] J. Sylvester and G. A. Uhlmann. A global uniqueness theorem for an inverse boundary value problem. *Ann. of Math. (2)*, 125(1):153–169, 1987.

[25] F. C. Trigo, R. Gonzalez-Lima and M. B. P .Amato, *Electrical Impedance Tomography using the Extended Kalman Filter*, IEEE Trans. Biomed. Engr., 51 (2004), pp. 72–81.

[26] G. A. Uhlmann, *Developments in inverse problems since Calderón's foundational paper*, Harmonic analysis and partial differential equations(Chicago, IL, 1996), Univ. Chicago Press, Chicago, IL, 1999.

[27] G. A. Uhlmann, *Commentary on Calderón's paper 28, On an inverse boundary value problem*, Selecta, edited by A. Bellow, C.E. Kenig, and P. Malliavin, to appear.

[28] G. Vainikko, Fast solvers of the Lippmann–Schwinger equation, in *Direct and Inverse Problems of Mathematical Physics* (Newark, DE), Kluwer Acad.¡ Publ, Dordrecht, Int. Soc. Anal. Appl. Comput. **5**, 423 (2000).